Monatshefte für Chemie 138, 1029–1034 (2007)
DOI 10.1007/s00706-007-0704-4
Printed in The Netherlands

Monatshefte für Chemie
Chemical Monthly

Molecular Dynamics Study on the Unbinding of *HBY 097* in the K103N Mutant *RT*

Luckhana Lawtrakul[1,*] and **Supa Hannongbua**[2]

[1] Department of Common and Graduate Studies, Sirindhorn International Institute of Technology (SIIT), Thammasat University, Pathum Thani, Thailand
[2] Department of Chemistry, Faculty of Science, Kasetsart University, Bangkok, Thailand

Received March 14, 2007; accepted April 24, 2007; published online July 20, 2007

Summary. The structural rearrangement due to the unbinding of *HBY 097* in K103N mutant HIV-1 reverse transcriptase (*RT*) was studied using two nanosecond molecular dynamics simulations. The simulations showed the dynamics of an open or upright position of the p66 thumb subdomain moving to a closed configuration together with the dynamic correction of protein residues around the non-nucleoside inhibitor binding pocket (NNIBP) and its putative entrance.

Keywords. Molecular dynamics simulations; HIV-1 reverse transcriptase; Non-nucleoside inhibitor; Virus mutation.

Introduction

In the human immunodeficiency virus type 1 (*HIV-1*) replication, a virus enzyme called reverse transcriptase (*RT*), synthesizes a double strand of *DNA* complementary to the virus *RNA*. This double-stranded *DNA* is then incorporated into the host cell's *DNA*; it directs the host cell machinery to produce copies of the virus. *RT* is a heterodimer composed of p66 and p51 subunits with identical amino acid sequences, but it differs in conformational rearrangements [1–4]. Generally, p66 resembles a human right hand and folds into four domains called fingers (residues 1–84 and 120–150), palm (residues 85–119 and 151–243), thumb (residues 244–322), and connection (residues 323–437), joined to the *RNase H* domain (residues 438–556), which is not present in p51 [5]. The polymerase catalytic site of the enzyme is specifically located on p66. Presently, 114 crystallographic structures of *HIV-1 RT* in various forms are contained in the *RCSB* Protein Data Bank (*RCSB* PDB) [6]. Some can distinguish between the different conformational states of *RT*, the free enzyme, *RT* bound to *RNA*/*DNA*, and *RT* bound to non-nucleoside inhibitors (NNIs) [4, 7–12]. These extend the understanding of the *RT* transcription mechanism and also the inhibition mechanisms of inhibitors. However, the drug-resistance mechanism by virus mutation is only partly known.

The X-ray structures provide information on the crystalline state, but, of course, contain no mobility data of biomolecules. One way to bring the biomolecular structures alive is molecular dynamics (MD) simulation, which provide dynamical properties in a solution on different timescales. All molecular modeling of the enzyme-substrate complexes have been based on the X-ray structures. The free energy calculations and the structural information from MD simulations have used advanced computer-assisted techniques in drug discovery and drug design [13–15]. Not many publications of studies of *RT* simulations have been presented because *HIV-1 RT* is a very large system. MD simulations of this enzyme require huge computer resources and rather long calculation times. All MD simulation results of *RT* [16–21] are in reasonable agreement with the assumption that NNIs inhibit enzyme activity by enlarging the *DNA*-binding cleft and limit the flexibility and mobility of the p66 thumb subdomain. This subdomain plays an important role in the translocation of the tem-

* Corresponding author. E-mail: luckhana@siit.tu.ac.th

plate-primer during *DNA* polymerization. However, a number of questions concerning the dynamics implications of the enzyme-inhibitor binding and the virus mutations in drug-resistance remain unanswered.

NNIs bind to a common hydrophobic pocket located in the palm subdomain of p66, 10 Å away from the polymerase catalytic site called the NNIs binding pocket (NNIBP). Drug resistant mutations are found for many residues, which are in close contact to NNIs (L100, K101, K103, V106, T107, V108, V179, Y181, Y188, V189, G190, F227, W229, L234, and Y318) and residues at the entrance of the binding pocket (P95, L100, K101, K103, V179, and Y181) [3, 9, 11]. Biochemical data indicate that K103N, Y181C, and Y188L *RT* mutations confer considerable drug resistance to most NNIs [10, 22–27]. The tyrosine amino acids (Y181C and Y188L) mutations involve loss of interactions between the protein and the bound inhibitor while asparagine amino acid (N103) of the K103N mutant *RT* acts as a gatekeeper controlling the entrance of the drug to the NNIBP [12, 28].

One recent paper has used a new methodology which uses constrained MD simulations *in vacuo* to predict NNIs (nevirapine) conformation in the K103N mutant *RT* [29]. Because of the short simulation time (0.175 ns) in a vacuum, this simulation shows a relatively poor fit when compared to the crystal structures. The present work studies 2 ns MD simulations of the K103N mutant *RT* unbinding process of *HBY 097* [(*S*)-4-isopropoxycarbonyl-6-methoxy-3-(methylthiomethyl)-3,4-dihydroquinoxalin-2(1*H*)-thione] in aqueous solution. *HBY 097* is an extremely potent second generation *NNRTI*, which potently inhibits both K103N ($EC_{50} = 3\,nM$) and Y181C ($EC_{50} = 2\,nM$) mutant *RTs* [30, 31]. The structural rearrangement and the motion of important residues at the NNIBP are investigated to gain more understanding of the inhibition mechanism of *HBY 097* in the K103N mutant *RT*.

Results and Discussion

Energy minimization was used to remove the inefficient contacts in the starting geometry, which were taken from X-ray structure and solvated with *TIP3P* water. The total energy after minimization is around $8.37 \times 10^4\,kJ\,mol^{-1}$ lower than that of the starting system.

This work was performed as a two-stage equilibration. In the first stage of equilibration, the system started at 100 K and gradually heated up to 300 K over 10 ps of simulation time with the volume held constant. Next, we equilibrated the system using pressure and temperature controls to adjust the density of water to the experimental value over 10 ps of simulation time. The temperature of the system was gradually increased over the 10 ps simulation time. It was 267.3 K, not exactly 300.0 K, but the temperature was close enough to be used in the next step. After equilibrating the system for 10 ps in stage 2, the system had a temperature 294.3 K and a density of $1.0\,g\,cm^{-3}$, *i.e.*, the experimental density of water. To guarantee that the system held these conditions, the simulation used 100 ps equilibration runs at constant temperature and constant pressure to reach equilibrium.

After the 120 ps equilibration, the conformation of the molecular system reached a stationary phase with a temperature of 298.6 K and a density of $1.0\,g\,cm^{-3}$. Finally, the whole system was equilibrated for 2 ns at 300 K with constant pressure using 2 fs time steps. The system properties that can be extracted from the data output files during 2 ns of MD simulation are energies, temperatures, pressures, volumes, and densities.

All energies increased during the first few ps, corresponding to heating the system from 100 to 300 K. The kinetic energy then remained constant for the remainder of the simulation, implying that the system's temperature, which acts on the kinetic energy, was in thermal equilibrium, and the system was working correctly. It remained within 2.7 K of 300 K for the remainder of the simulation. The potential energy, and consequently the total energy initially increased and then remained constant for the remainder of the simulation, indicating that the relaxation was completed and that an equilibrium was reached at a density of $1.0\,g\,cm^{-3}$.

In the MD simulation, the system started from a non-equilibrium state, since the X-ray structure corresponds to a K103N mutant *RT* in complex with *HBY 097*, while the inhibitor was removed in the simulation. We expected to see the movement of the p66 *RT* subdomains during these simulations due to the ligands absence in the NNIBP.

The root mean square deviations (*RMSD*) of the C_α atoms of the whole 437 amino acid residues as a function of the simulation time are shown in Fig. 1. The average *RMSD* of the trajectories during the simulations were aligned based on the C_α atoms from the X-ray structure of the K103N mutant *RT*/

HBY 097 complex (PDB code 1HQU) [12] and the X-ray structure of the K103N mutant *RT* (PDB code 1HQE) [12] and are 3.99 and 9.07. This shows that the trajectories from our MD simulation are more similar to the starting structure (1HQU) than the expected structure (1HQE). These trajectories provide mobility information of *RT* during the NNI binding and unbinding processes. The overall structural differences of p66 of (i) the starting X-ray structure K103N mutant *RT*/*HBY 097* complex (1HQU); (ii) X-ray structure of the K103N mutant *RT* (1HQE); and (iii) the average structure from MD simulations are presented in Fig. 2. The crystal structure of K103N mutant *RT* without inhibitor is in a closed conformation

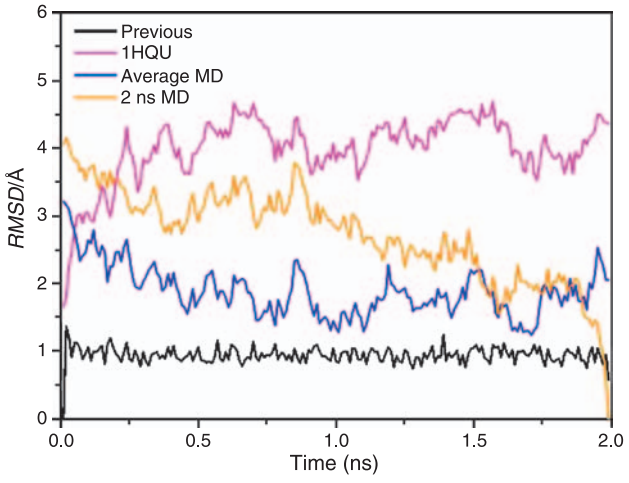

Fig. 1. Root mean square deviations (*RMSD*) (Å) of C_α atoms as a function of simulation time. All structures were aligned based on the C_α atoms with: (i) the 10 ps previous structures (black line); (ii) the X-ray structure of the K103N *RT*/*HBY 097* (1HQU) (magenta line); (iii) the average structure during 2 ns simulation (blue line); and (iv) the structure at 2 ns simulation (orange line)

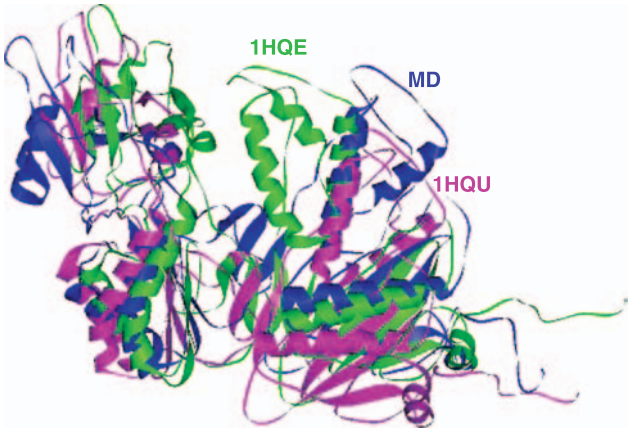

Fig. 2. Superposition showing the orientation of the p66 thumb subdomain. The X-ray structures of the K103N *RT* (1HQE), K103N *RT*/*HBY 097* (1HQU), and the average structure during 2 ns MD simulation are represented in green, magenta, and blue ribbons

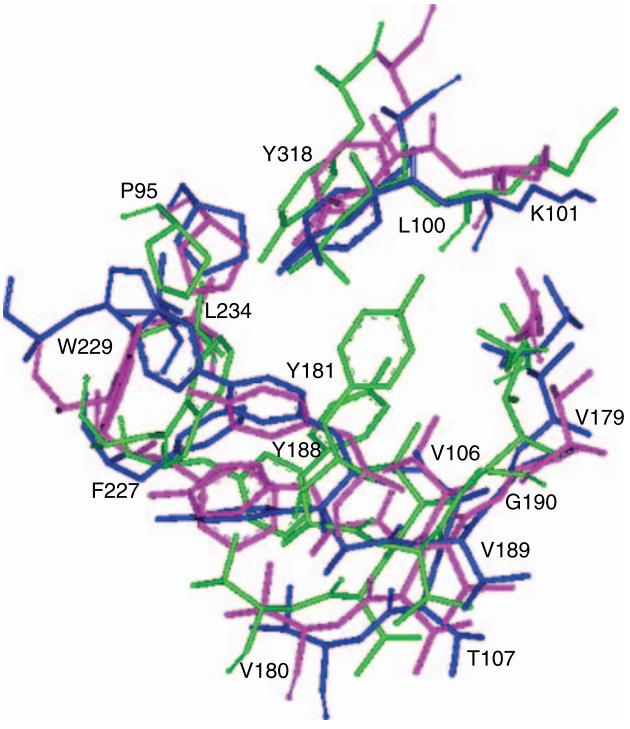

Fig. 3. Schematic diagram showing superposition of NNIBP and the amino acid residues at the entrance of the binding pocket between crystal structures of K103N *RT* (1HQE; green sticks) and K103N *RT*/*HBY 097* (1HQU; magenta sticks) together with the average structure during 2 ns simulation (MD; blue sticks)

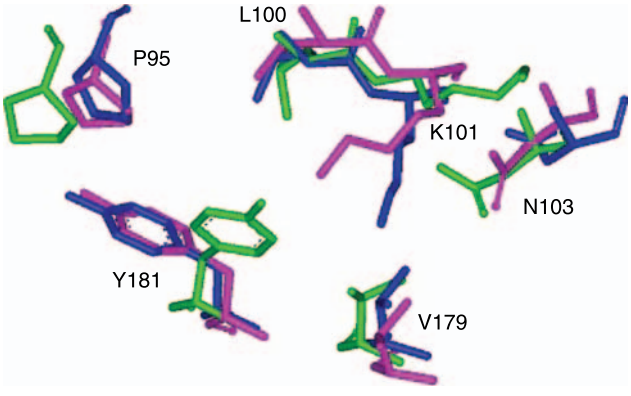

Fig. 4. Superposition showing the orientation of amino acid residues at the entrance of NNIBP (P95, L100, K101, K103N, V179, and Y181). Crystal structures of K103N *RT* (1HQE), K103N *RT*/*HBY 097* (1HQU), and the average structure during 2 ns simulation (MD) are represented in green, magenta, and blue sticks

Table 1. Root mean square deviations (*RMSD*) of C_α atoms (16 atoms), back-bone atoms (94 atoms), and all atoms (280 atoms) of amino acid residues at NNIBP and the putative entrance (P95, L100, K101, K103N, V106, T107, V108, V179, Y181, Y188, V189, G190, F227, W229, L234, and Y318)

RMSD / Å	C_α			Back-bone			All atoms		
	1HQE	1HQU	MD	1HQE	1HQU	MD	1HQE	1HQU	MD
1HQE	0.00	1.03	1.66	0.00	1.07	1.75	0.00	2.52	2.94
1HQU	1.03	0.00	1.01	1.07	0.00	1.16	2.52	0.00	1.57
MD	1.66	1.01	0.00	1.75	1.16	0.00	2.94	1.57	0.00

when compared to the K103N in complex with the *HBY 097* structure. These differences point to the gap between finger and thumb subdomains. The average structure from the MD simulations point to the right up translation as expected. This motion occurs because of the unbinding of *HBY 097*. The structures of the residues composing the NNIBP and the entrance of the pocket are shown in Fig. 3.

Upon loss of interaction with NNI, the residues rearrange to reduce the volume inside the pocket. The major portions that can be clearly seen in Fig. 3 are the motion of the aromatic tyrosine rings (Y181, Y188, and Y318), F227, and W229. Generally, the average NNIBP structure from the simulation is more similar to the starting structure (*RT*/*HBY 097* complex) than to the free enzyme as shown in Fig. 3 and Table 1. These imply that the 2 ns simulation run is not of sufficient length for the translocation correction of all protein residues at NNIBP. However, a number of adjustments in the average conformation of NNIBP and the putative entrance residues may partially compensate for the loss of inhibitor interaction. As shown in Fig. 4, the orientations of K101, K103N, and V179, which act as the gatekeepers controlling the entrance of the drug to the NNIBP and the side chains of K101 and K103N, are quite flexible while V179 in three different structures does not vary much. The putative entrance residues have high movement capability upon removal of the *HBY 097* inhibitor.

The hydrogen bond distances of amino acid residues at the NNIBP and the putative entrance are presented in Fig. 5A–C and Table 2. The hydrogen bond of N103–K101 (ND2-O) in *HBY 097* binding structure is lost in the average structure of MD simulations and in the free enzyme (1HQE) conformation. During the *HBY 097* unbinding process the hydrogen bond distance of V179 N–O G190 decreases while in G190 N–O V179, it increases. These point out that hydrogen bonds of V179–G190 (N–O and O–N) are significant in the *RT*/*HBY 097* complex. The hydrogen bonds between these amino acids stabilize the putative entrance and the NNIBP in an active shape, which compensates for the loss of the K103N interaction. This may explain why *HBY 097* is still a potent inhibitor in the K103N *RT* mutant structure.

Table 2. Distances of hydrogen bonds of amino acid residues at NNIBP and the putative entrance (P95, L100, K101, K103N, V106, T107, V108, V179, Y181, Y188, V189, G190, F227, W229, L234, and Y318)

	Distance/Å		
	1HQE	1HQU	MD
N103 ND2-O K101	N/H	2.92	N/H
T107 N-O V189	2.92	2.73	2.80
V179 N-O G190	N/H	3.14	2.95
Y181 N-O Y188	2.85	N/H	2.99
Y188 N-O Y181	2.83	3.16	2.80
V189 N-O T107	2.82	2.60	2.90
G190 N-O V179	2.89	2.89	3.12
F227 N-O L234	3.16	3.02	3.04
W229 NE1-O P95	N/H	N/H	2.85
L234 N-O F227	2.86	2.86	2.89

N/H is no hydrogen bond

Methods

Molecular Model

All of the MD simulations were performed with the AMBER 7 program [32] using the *ff99* force field running on a 3 GHz processor of a Dell model Optiplex GX260 Mini Tower computer. The graphical displays were generated with the WebLab ViewerPro 4.0 [33] software program. The simulation models were constructed based on the X-ray structures of K103N mutant *HIV-1 RT* (PDB code 1HQE), while the inhibitor was removed before the simulation. The entire structure of *HIV-1 RT* was too large to be simulated by our current computational facilities. Structural and biochemical data indicate that the NNIBP is mainly composed of structural elements of the p66 subunit, and that the *RNase H* subdomain and the p51 subunit are not directly involved in NNI binding, and play a minor role in the sensitivity to NNIs. Therefore in the present

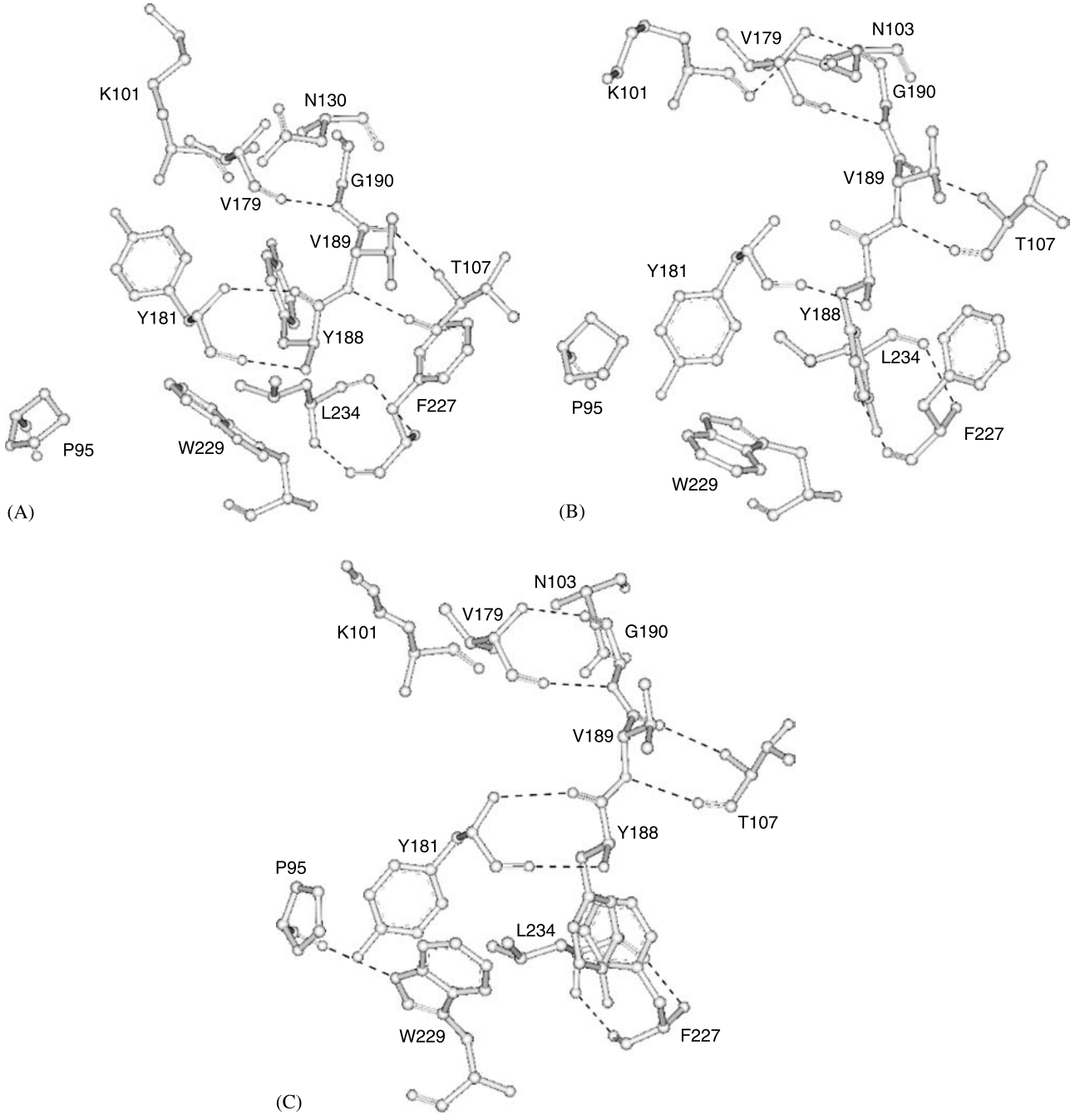

Fig. 5. Schematic diagrams representing the hydrogen bonding (black dashed lines) between amino acid residues of NNIBP and the entrance of the binding pocket. (A) K103N *RT* (1HQE), (B) K103N *RT/HBY 097* complex (1HQU), and (C) the average structure during 2 ns simulation (MD)

simulation study, both *RNase H* and the p51 subunit were omitted to facilitate the simulation and save computation time. The *tleap* module of AMBER added the hydrogen atoms and some side chains with missing coordinates. The simulation model was solvated into a truncated octahedral 18.77 $Å^3$ box of *TIP3P* water. The system required Cl^- as counter ions to complete the model. In total, the simulation system contains 7244 protein atoms, 4 Cl^- counter ions, and 103278 atoms from water molecules.

Molecular Dynamics Simulation

The whole system was first energy-minimized by the *Sander* module of AMBER using 200 steps of steepest descent, followed by 1500 steps for conjugate gradient to reduce steric conflicts between water molecules and the protein. Solvent equilibration was performed in a two-stage equilibration. In the first stage, the system was started from a temperature of 100 K and gradually heated up to 300 K over 10 ps of simulation time with the volume held constant. Next, the system was

equilibrated using pressure and temperature controls at 300 K over 10 ps to adjust the density of water to experimental values. Then these conditions were used to continue through 100 ps to equilibration. Finally, the whole system was equilibrated for 2 ns at 300 K with constant pressure using 2 fs time steps.

Acknowledgements

We are grateful to *Prof. Dr. Peter Wolschann* for helpful discussions and *Paul V Neilson* for carefully reading through the manuscript. We would like to thank the Thailand Research Fund (*TRF*) for financial support of the *HIV-1 RT* work with grants to *L. Lawtrakul* (MRG4680111) and *S. Hannongbua* (BRG4780007).

References

[1] Kohlstaedt LA, Wang J, Friedman JM, Rice PA, Steitz TA (1992) Science **256**: 1783
[2] Jacobo-Molina A, Clark AD Jr, Williams RL, Nanni RG, Clark P, Ferris AL, Hughes SH, Arnold E (1991) Proc Natl Acad Sci USA **88**: 10895
[3] Tantillo C, Ding J, Jacobo-Molina A, Nanni RG, Boyer BL, Hughes SH, Pauwels R, Andries K, Janssen PA, Arnold E (1994) J Mol Biol **243**: 369
[4] Ding J, Das K, Tantillo C, Zhang W, Clark AD Jr, Jessen S, Lu X, Hsiou Y, Jacobo-Molina A, Andries K, Pauwels R, Moereels H, Koymans L, Janssen PAJ, Smith RH Jr, Kroeger Koepke M, Michejda CJ, Hughes SH, Arnold E (1995) Structure **3**: 365
[5] Rodgers DW, Gamblin SJ, Harris BA, Ray S, Culp JS, Hellmig B, Woolf DJ, Debouck C, Harrison SC (1995) Proc Natl Acad Sci USA **92**: 1222
[6] Bermann HM, Westbrook J, Feng Z, Gilliland G, Bhat TN, Weissig H, Shindyalov IN, Bourne PE (2000) Nucleic Acids Res **28**: 235
[7] Ding J, Das K, Moereels H, Koymans L, Andries K, Janssen PA, Hughes SH, Arnold E (1995) Nat Struct Biol **2**: 407
[8] Wang J, Smerdon SJ, Jager J, Kohlstaedt LA, Rice PA, Friedman JM, Steitz TA (1994) Proc Natl Acad Sci USA **91**: 7242
[9] Ren J, Esnouf RM, Garman E, Somers D, Ross C, Kirby I, Keeling J, Darby G, Jones Y, Stuart D, Stammers D (1995) Nat Struct Biol **2**: 293
[10] Das K, Ding J, Hsiou Y, Clark AD Jr, Moereels H, Koymans L, Andries K, Pauwels R, Janssen PA, Boyer PL, Clark P, Smith RH Jr, Kroeger Smith MB, Michejda CJ, Hughes SH, Arnold E (1996) J Mol Biol **264**: 1085
[11] Hsiou Y, Ding J, Das K, Clark AD Jr, Hughes SH, Arnold E (1996) Structure **4**: 853
[12] Hsiou Y, Ding J, Das K, Clark AD Jr, Boyer PL, Lewi P, Janssen PA, Kleim JP, Rosner M, Hughes SH, Arnold E (2001) J Mol Biol **309**: 437
[13] Mc Cammon JA, Gelin BR, Karplus M (1977) Nature **267**: 585
[14] Duan Y, Kollman PA (1998) Science **282**: 740
[15] Hansson T, Oostenbrink C, van Gunsteren WF (2002) Curr Opin Struc Biol **12**: 190
[16] Eriksson MAL, Pitera J, Kollman PA (1999) J Med Chem **42**: 868
[17] Weinzinger P, Hannongbua S, Wolschann P (2005) J Enzym Inhib Med Chem **20**: 129
[18] Wang J, Morin P, Wang W, Kollman PA (2001) J Med Chem **123**: 5221
[19] Shen L, Shen J, Luo X, Cheng F, Xu Y, Chen K, Arnold E, Ding J, Jiang H (2003) Biophys J **84**: 3547
[20] Zhou Z, Madrid M, Evanseck JD, Madura JD (2005) J Am Chem Soc **127**: 17253
[21] Smith RH Jr, Jorgensen WL, Tirado-Rives J, Lamb ML, Janssen PAJ, Michejda CJ, Smith MBK (1998) J Med Chem **41**: 5272
[22] Ding J, Das K, Hsiou Y, Sarafianos SG, Clark AD Jr, Jacobo-Molina A, Tantillo C, Hughes SH, Arnold E (1998) J Mol Biol **284**: 1095
[23] Byrnes VW, Emini EA, Schleif WA, Condra JH, Schneider CL, Long WJ, Wolfgang JA, Graham DJ, Gotlib L, Schlabach AJ, Wolanski BS, Blahy OM, Quintero JC, Rhodes A, Roth E, Titus DL, Sardana VV (1994) Antimicrob Agents Chemother **38**: 1404
[24] Richman DD (1993) Antimicrob Agents Chemother **37**: 1207
[25] de Clercq E (1998) Antiviral Research **38**: 153
[26] Rübsamen-Waigmann H, Huguenel E, Shah A, Paessens A, Ruoff HJ, von Briesen H, Immelmann A, Dietrich U, Wainberg MA (1999) Antiviral Research **42**: 15
[27] Kleim JP, Winters M, Dunkler A, Suarez JR, Riess G, Winkler I, Balzarini J, Oette D, Merigan TC (1999) J Infect Dis **179**: 709
[28] Das K, Sarafianos SG, Clark AD Jr, Boyer PL, Hughes SH, Arnold E (2007) J Mol Biol **365**: 77
[29] Garner J, Deadman J, Rhodes D, Griffith R, Keller PA (2007) J Mol Graph Model (doi: 10.1016/j.jmgm.2006.11.004)
[30] Kleim JP, Bender R, Kirsch R, Meichsner C, Paessens A, Rosner M, Rubsamen-Waigmann H, Kaiser R, Wichers M, Schneweis KE (1995) Antimicrob Agents Chemother **39**: 2253
[31] Balzarini J, Pelemans H, Riess G, Roesner M, Winkler I, de Clercq E, Kleim JP (1998) Biochem Pharmacol **55**: 617
[32] Case DA, Pearlman DA, Caldwell JW, Cheatham III TE, Wang J, Ross WS, Simmerling CL, Darden TA, Merz KM, Stanton RV, Cheng AL, Vincent JJ, Crowley M, Tsui V, Gohlke H, Radmer RJ, Duan Y, Pitera J, Massova I, Seibel GL, Singh UC, Weiner PK, Kollman PA (2002) AMBER7, University of California, San Francisco
[33] Molecular Simulations Inc. (2000) WebLab ViewerPro 4.0, Molecular Simulations Inc., San Diego

Verleger: Springer-Verlag GmbH, Sachsenplatz 4–6, 1201 Wien, Austria. – Herausgeber: Österreichische Akademie der Wissenschaften, Dr.-Ignaz-Seipel-Platz 2, 1010 Wien, und Gesellschaft Österreichischer Chemiker, Eschenbachgasse 9, 1010 Wien, Austria. – Redaktion: Getreidemarkt 9/163-OC, 1060 Wien, Austria. – Satz und Umbruch: Thomson Press Ltd., Chennai, India. – Offsetdruck: Krips bv, Kaapweg 6, 7944 HV Meppel, The Netherlands. – Verlagsort: Wien. – Herstellungsort: Meppel. – Printed in The Netherlands.